Journal of Thermal Analysis and Calorimetry, Vol. 82 (2005) 409–415

THERMOANALYTICAL CHARACTERIZATION OF VANADIUM–CHROMIUM OXIDE COMPOUNDS PREPARED BY 'SOFT CHEMISTRY' METHOD

O. Pozdnyakova[1], *J. Megyeri*[1], *E. Kuzmann*[2] *and L. Szirtes*[1*]

[1]Institute of Isotopes, Chemical Research Center of the Hungarian Academy of Sciences, P.O. Box 77, 1525 Budapest, Hungary
[2]Department of Nuclear Chemistry, Research Group of Nuclear Methods in Structural Chemistry HAS, Eötvös Lorand University, P.O. Box 32, 1518 Budapest, Hungary

Hydrated microcrystalline compound, $V_{1-x}Cr_xO_y{\cdot}nH_2O$, where $x<0.063$ and $4.4<n<8$ and hydrated amorphous phases, $CrVO_4{\cdot}H_2O$ and $Cr_2V_4O_{13}{\cdot}4H_2O$ have been prepared using peroxo-polyacids of vanadium and chromium. The transformations of these hydrated phases upon heating were studied by TG-DTA and XRD techniques and led to three crystalline anhydrous compounds: (*i*) phase $V_{1-x}Cr_xO_y$, which is closely related to the orthorhombic V_2O_5, (*ii*) $Cr_2V_4O_{13}$ and (*iii*) monoclinic $CrVO_4$–M. The ranges of coexistence of phases in equilibrium were also determined.

Keywords: *chromium, sol–gel, thermal analysis, vanadium*

Introduction

Mixed vanadium–chromium oxide compounds present a wide range of interesting properties; for instance, they have excellent catalytic properties [1–9], and recently they were shown to be potential candidates for anodes in lithium-ion batteries [10].

These compounds may be synthesised at high temperatures via ceramic route or through 'soft chemistry' route. Among the main 'soft chemistry' routes used for the preparation of vanadium-based oxides are the sol–gel, hydrothermal, and co-precipitation routes. The former that allows a good control of the synthesis was used for the preparation of Cr-doped V_2O_5 xerogels [11]. Co-precipitation methods, under specified pH conditions, were applied to the synthesis of $CrVO_4{\cdot}nH_2O$ [12, 13], $Cr_2V_4O_{13}{\cdot}nH_2O$ [12], $Cr(VO_3)_3{\cdot}nH_2O$ [14], $(CrOH)_xV_{12-y}Cr_yO_m{\cdot}nH_2O$ [15] and $Cr_4(V_2O_7)_3{\cdot}nH_2O$ [16] compounds. By appropriate annealing of the usually amorphous hydrated phases, several crystalline vanadates were obtained as well [11–14, 16, 17]. We have recently reported on a novel aqueous method used to synthesise mixed oxide hydrate, $V_{1-x}Cr_xO_y{\cdot}nH_2O$, via the reaction of peroxo-polyacids of vanadium and chromium [18]. In the present work, this method was employed to study in more detail the V^{5+}–Cr^{3+}–O system. Differential thermal analysis (DTA), thermogravimetry (TG) and powder X-ray diffraction analyses were applied to monitor dehydration/crystallisation and phase transition processes upon heat treatment of the hydrated vanadates obtained through the reaction of peroxo-polyacids of vanadium and chromium and determine the ranges of coexistence of the phases in equilibrium.

Experimental

Series of samples with Cr/V atomic ratio, z in the range of $0.008 \le z \le 3$ were synthesised from the reaction of peroxo-polyacids of vanadium and chromium according to the procedure as described earlier [18]. Vanadium/chromium ratios in the resulting compounds were verified by means of ICP (GBC-Integra XM) analysis. Based on the analytical data, the samples investigated can be considered as the combination V_2O_5–yCr_2O_3 where $0.008 \le y \le 3$ (Table 1).

The X-ray powder diffraction study was performed with a Bragg–Brentano geometry, using powder samples with a Philips PW-1050/25 powder diffractometer (at 45 kV and 35 mA) with CuK_α radiation and graphite monochromator. The powder diffraction patterns were scanned by steps of 0.01° (2θ), with fixed accounting times (20 s). The diffractograms were evaluated using EXRAY program [19].

Thermoanalytical investigations were carried out for samples of 50 mg mass in air at heating rate of 10 K min^{-1} by means of a Mettler TA-1HT computer controlled thermobalance that simultaneously provided DTA and TG data. The onset temperatures, obtained from the first derivative of the DTA curve, were taken as transformation temperatures, the accuracy be-

* Author for correspondence: szirtes@iki.kfki.hu

1388–6150/$20.00

Akadémiai Kiadó, Budapest, Hungary
Springer, Dordrecht, The Netherlands

Table 1 Nominal and actual compositions of the samples studied

Nominal values			Measured values
V_2O_5/ mol%	Cr_2O_3/ mol%	Cr/V ratio, *z*	Cr/V ratio, *z*
99.187	0.813	0.0082	0.0081
97.500	2.500	0.0256	0.0259
95.833	4.167	0.0435	0.0433
93.750	6.250	0.0667	0.0672
91.667	8.333	0.0909	0.0913
87.500	12.50	0.1429	0.1430
83.333	16.667	0.2000	0.1992
79.167	20.833	0.2632	0.3257
75.000	25.000	0.3333	0.3367
70.588	29.412	0.4167	0.4170
66.667	33.333	0.4999	0.4902
58.333	41.667	0.7143	0.7246
50.000	50.000	1.0000	0.9968
33.333	66.667	2.0000	2.0013
25.000	75.000	3.0000	3.0488

ing ±3 K. For selected samples, under the same conditions, thermoanalytical investigations were carried out by means of a Derivatograph C type instrument (Hungarian Optical Works, Budapest) connected to selective water detector [20].

Results and discussion

The XRD patterns of the as-prepared samples are featureless indicating amorphous nature of the powders. The transition from amorphous to crystalline state takes place between 573 and 773 K depending on the initial composition of the samples. As discussed in details further on, thermoanalytical investigations revealed significant differences in thermal behavior of the as-prepared samples depending on their Cr/V atomic ratio, *z* (Fig. 1). Regarding to the initial sample composition, four domains with similar DTA-TG-DTG patterns can be distinguished:

- samples with $z \leq 0.067$ (domain I)
- samples with $0.067 < z \leq 0.5$ (domain II)
- samples with $0.5 < z \leq 1$ (domain III)
- samples with $z > 1$ (domain IV)

To understand the phase transitions evidenced by DTA, XRD analyses have been performed for samples annealed under air flow at various temperatures on both sides of the thermal effects observed and quenched by removing the samples from the furnace at the annealing temperature.

Domain I

DTA, TG and DTG curves for samples with $z \leq 0.067$ are presented in Fig. 1a. In this domain, as-prepared samples contain about 80 mass% of water (calculated from the total mass loss), their dehydration takes place in three steps (Table 2) in 303–398, 403–473 and 553–603 K temperature ranges followed by crystallisation and melting of the resulting compound at 928 K. The mass loss below 473 K is accompanied by two broad overlapped endothermic peaks. The final mass loss is correlated with a small endothermic peak immediately followed by crystallisation exotherm. It has been observed that upon increasing Cr/V ratio in the samples the endothermic process of the structural water loss became more prolonged, taking place in the temperature interval up to 626 K. Consequently, the samples' crystallisation temperature increases with increasing Cr/V ratio from 548 K (z=0.008) to 626 K (z=0.067). The fact that exothermic peak in the differential thermal curves corresponding to crystallisation of the samples is single and relatively sharp suggests that our preparations are not a simple mixture of deriv-

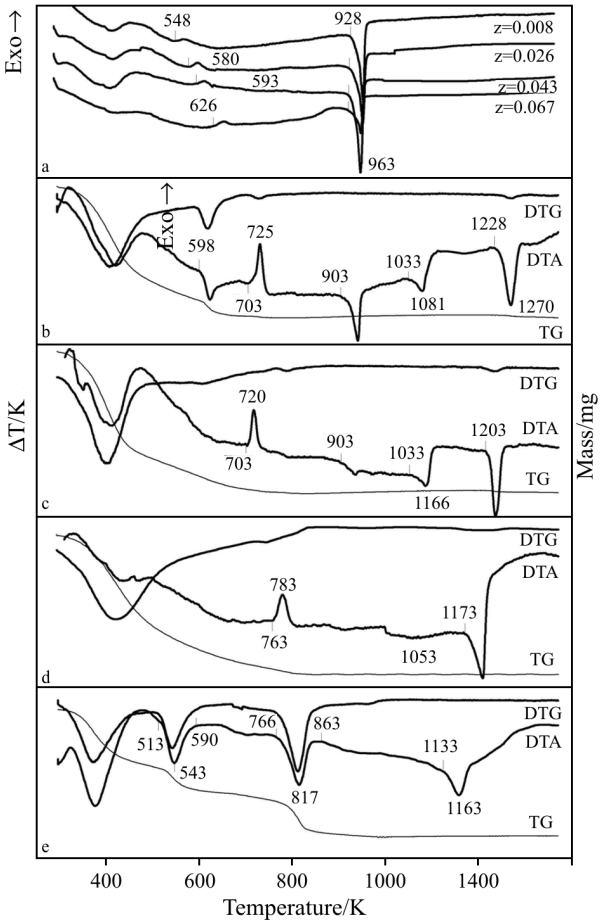

Fig. 1 DTA curves of samples with a – $z \leq 0.067$ and DTA-DTG-TG curves of samples with b – z=0.337, c – 0.490, d – 0.997 and e – 3.049

Table 2 Mass losses and water content of samples with $z \leq 0.067$

Cr/V ratio, z	Mass loss below 473 K/%		Mass loss before crystallization/%	Total water content/mol H_2O/mole Cr
	1st step	2nd step	3rd step	
0.0081	41.21	39.43	19.36	4.36
0.0259	42.93	37.41	19.66	5.14
0.0433	39.67	39.22	21.11	6.75
0.0672	40.92	34.92	24.16	7.89

atives based on each constituent metal oxide, but a distinct amorphous-like compound.

Based on the analytical data and TG measurements, the general composition of the mixed oxide hydrate can be expressed as $V_{1-x}Cr_xO_y \cdot nH_2O$, where $x<0.063$ and $4.4<n<8$. It should be noted that in the present study the region of $V_{1-x}Cr_xO_y \cdot nH_2O$ compound homogeneity was determined more precisely, while chromium content of this hydrate communicated in our preliminary study [18] was overestimated.

The general profile of the X-ray diffractograms for the as-prepared hydrate $V_{1-x}Cr_xO_y \cdot nH_2O$ is characteristic of microcrystalline, amorphous-like material (Fig. 2). The patterns of the as-prepared samples are peculiar in the broad asymmetrical peak shape, rising very rapidly and then decreasing continuously toward high angle side. Every reflection peak coincides in the 2θ position with the (*hk*0) reflections of orthorhombic V_2O_5 except for a strong peak at about 8 and a weak one at 23.1° As has been pointed out [21], these features might suggest a random layer structure which consists of layers (*a*–*b*) arranged parallel and equidistant, but random in translation parallel to the layer and rotation about the normal (*c*).

As has been demonstrated in our previous work [18], microcrystalline $V_{1-x}Cr_xO_y \cdot nH_2O$ compound shows some structural periodicity corresponding to the basal spacing of ca. 1.088–1.146 nm. The structural

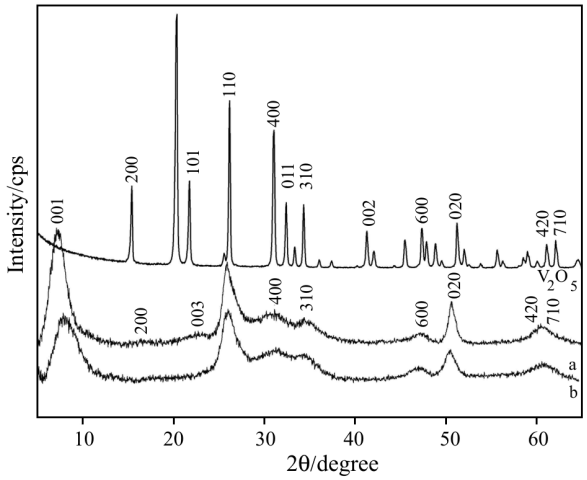

Fig. 2 X-ray diffraction patterns of samples with a – z=0.043 and b – 0.067 and orthorhombic V_2O_5

features of this vanadium–chromium oxide material were examined and discussed in comparison with those exhibited by the parent oxide V_2O_5 and V_2O_5 xerogel [18]. It has been proposed that its structural framework might be similar to that of the later one.

The increase in the thermal stability of the preparations upon increasing Cr content could be associated with the enhanced degree of disorder induced by the guest chromium cations observed upon increasing Cr/V ratio in the samples [18]. Apparently, water molecules could be more readily removed from samples with less chromium content. A random orientation of smaller two-dimensional crystallites probably introduces some diffusional limitations which could affect the DTG-DTA curves for the 'less layered' more amorphous samples with higher chromium content. The kinetic factors associated with the leave of increasing amount of water under conditions of constant heating rate might have also affected the DTA traces observed.

According to the TG-DTA and XRD results, the transformation from two-dimensional amorphous-like hydrate to crystalline anhydrous phase is characterised by three steps of dehydration and crystallisation. The first two steps were ascribed to the release of physically absorbed and interlayer water, respectively. The origin of the third step was not unambiguously assigned. It could be associated with the leave of water molecules coordinated to Cr^{3+} ions or further dehydration of the V–O layers [22–24].

Figure 3 shows the evolution of the X-ray diffraction patterns as a function of the annealing temperature for sample with z=0.043. The X-ray data of the compound annealed at 553 K show the beginning of crystallisation (consistent with the thermal measurement), while when annealed at 603 K a well-crystallised compound was obtained. The crystalline phase obtained after annealing the hydrate at the temperatures just above the exothermic peaks on corresponding DTA curves expressed XRD pattern very similar to that one of the orthorhombic V_2O_5 (Fig. 3). It should be noted that successive grindings had to be performed prior to XRD analysis to minimise effects of particles preferential orientation. The precise structural refinement of this crystalline phase has not been performed yet. It has been proposed, however, that structural periodicity of the $V_{1-x}Cr_xO_y \cdot nH_2O$ hydrate might be associated with the

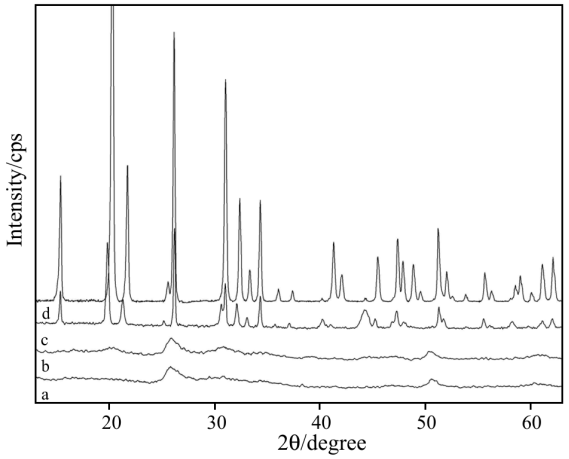

Fig. 3 X-ray diffraction patterns of sample with z=0.043 annealed at a – 473, b – 553 and c – 603 K and d – orthorhombic V_2O_5

formation of polyelement oxide network incorporating both V and Cr in the same crystallographical site [18]. After annealing the hydrate, somewhat similar structure might be preserved and formation of topotactic substitutional solid solution-type material might take place. This assumption correlates with the findings of Volkov *et al*. [25, 26] who have reported on the formation of $(V_{1-x}T_x)_2O_{5+y}$ (T=Mo, W) complex oxide upon heat treatment of the parent $H_2V_{12-x}T_xO_{31+y}\cdot nH_2O$ compound and of Dupont *et al.* [27, 28] on the phase transition mechanisms from hydrated mixed vanadium–molybdenum (tungsten) oxide precursors synthesised by chimie douce to the metastable and stable product $V_xT_{1-x}O_{3-y}$ (T=Mo, W).

On the other hand, Gregorie *et al*. [11] have reported on the synthesis of the mixed oxide $Cr_{0.11}V_2O_{5.16}$ by annealing the parent $Cr_xV_2O_5\cdot nH_2O$ xerogel at 793 K, which was obtained from vanadium oxide gel by ionic exchange from $Cr(NO_3)_3$ solution. The structure of this bronze, determined by Rietveld refinement, was proposed to encompass the V_2O_5 framework with a localisation of the Cr^{3+} ion in the quasi-square plane formed by the four oxygen atoms of the V_2O_5 slab. The results of the DSC and TG measurements reported by Gregorie *et al*. for the $Cr_{0.11}V_2O_{5.16}$ compound are very similar to that ones reported here for the $V_{1-x}Cr_xO_y\cdot nH_2O$, x<0.063, preparations. Therefore, even though the different synthesis procedure was applied, the possibility of formation of interstitial solid solution upon annealing the $V_{1-x}Cr_xO_y\cdot nH_2O$ hydrate is to be considered.

More detailed TG-DTA and high temperature XRD characterisation of the phase transition process from two-dimensional amorphous-like $V_{1-x}Cr_xO_y\cdot nH_2O$ hydrate to anhydrous crystalline phase and results of the studies on the possible structure of the later one will be reported in other publication [29].

Domain II

With the increase of chromium content beyond the Cr/V molar ratio of 0.067, DTA-TG curves follow the same pattern as described earlier except for no further increase of the crystallisation temperature of the samples is observed and large melting endotherm, present up to z<0.5, shifts abruptly from 928 to 903 K (Fig. 1b). The exothermic peak corresponding to the crystallisation of $V_{1-x}Cr_xO_y$ phase progressively decreases, became poorly resolved (z=0.337) and diminishes completely with further increase of Cr/V molar ratio (z=0.417). Instead, new exothermic peak appears at ca. 703 K and becomes well resolved starting from sample with z=0.337.

The exothermic peak at ca. 703 K corresponds to the crystallisation of $Cr_2V_4O_{13}$ phase [12], which was confirmed by X-ray analysis performed upon the $0.337<z\leq0.5$ samples annealed at 773 K. The intensity of the Bragg's reflections corresponding to the monoclinic $Cr_2V_4O_{13}$ (JCPDS 46-0061) increases and those of $V_{1-x}Cr_xO_y$ decreases with increasing Cr/V molar ratio in the samples, in consistency with the variation of the ratio of the phases present as evidenced by DTA-TG measurements. At z=0.49 the preparation mainly consisted of amorphous $Cr_2V_4O_{13}\cdot 4H_2O$ phase, which thermal behaviour (Fig. 1c) can be summarised as follows:

$$Cr_2V_4O_{13}\cdot 4H_2O \text{ amorph.}\rightarrow Cr_2V_4O_{13} \text{ amorph.}\rightarrow$$
$$\rightarrow Cr_2V_4O_{13} \text{ cryst.}\rightarrow CrVO_4\text{–}O+V_2O_5$$

Indeed, in addition to the exothermic peak at ca. 703 K, all DTA curves in the $0.067<z\leq0.5$ domain of samples composition exhibit two endothermic effects: at ca. 1033 K and in the temperature interval of 1173–1228 K. In accordance with the XRD data, the effect at ca. 1033 K was assigned to the decomposition of $Cr_2V_4O_{13}$ phase that melts incongruently depositing $CrVO_4$ and at 1228 K one – to the incongruent melting of thus formed orthorhombic $CrVO_4$. With increasing Cr/V ratio in the samples, the onset of the second endotherm shifts to lower temperatures and reaches its minimum at 1173 K for z=1.

The melting point of $CrVO_4$ has not been unambiguously established so far. The various authors give 1083 [30], 1133 [31], 1159 [32], 1175 [33, 34] and 1190 K [35]. The discrepancies between the literature data could probably be associated with the observed shift of the endotherm assigned to the melting of $CrVO_4$ phase, depending on the Cr/V ratio in the preparations. This phenomenon, which even thought evident from the experimental DTA points depicted on phase diagrams given by some authors [31, 34], was not referred to in earlier works [30–35] and suggests a need for further study.

Domain III

For the preparations with $0.5<z\leq1$, additional thermal phenomena appeared on the DTA curves: large exothermic peak at 763 K and two endothermic peaks in the temperature intervals of 1053–1163 and 1173–1228 K (Fig. 1d). In consistency with the XRD data, the first effect corresponds to the crystallisation of monoclinic chromium orthovanadate, $CrVO_4$–M followed by monotropic transformation in the temperature interval of 1053–1163 K that leads to orthorhombic chromium orthovanadate, $CrVO_4$–O. The later one melts incongruently in the temperature interval of 1173–1228 K as described earlier.

Indeed, XRD analysis of the preparation with z=0.997 annealed at 823 K showed the presence of $CrVO_4$–M phase. The evolution of the X-ray diffraction patterns as a function of the annealing temperature for sample with z=0.997 is shown in Fig. 4. From 323 to 723 K, the sample is amorphous but upon increasing the annealing temperature up to 823 K, we obtained the X-ray signature of the monoclinic $CrVO_4$ phase (JCPDS 83-0761). This monoclinic phase is maintained upon further heating to 973 K, but converts progressively to the orthorhombic $CrVO_4$ phase when the annealing temperature reaches 1073 K. The thermal behaviour of this preparation resembled that one of $CrVO_4{\cdot}nH_2O$ obtained using other aqueous methods [12, 13] and can be summarised as follows:

$$CrVO_4{\cdot}H_2O \text{ amorph.} \rightarrow CrVO_4 \text{ amorph.} \rightarrow$$
$$\rightarrow CrVO_4\text{–M cryst.} \rightarrow CrVO_4\text{–O cryst.}$$

The later process is reflected on the DTA curves as a broad endotherm at ca. 1053 K (z=0.997) or as a sharp endotherm at 1163 K (z=0.725). Increase in the temperature of M to O transition at $z<1$ is probably associated with the presence of another phase, $Cr_2V_4O_{13}$, which undergoes incongruent decomposition in the same temperature interval.

Domain IV

New thermal effects all accompanied by mass losses were observed for samples with $z>1$, as evidenced by TG-DTG-DTA curves: well resolved endotherm at 513 K, poorly resolved endotherm at ca. 573 K and broad endothermic feature consisting of several overlapped and poorly resolved peaks in the temperature interval of ca. 848–993 K. The endothermic effects in the temperature interval of ca. 848–993 K became more pronounced for samples with $z\geq2$.

These endothermic effects and associated mass losses might be attributed to the simultaneous decomposition of hydrated complex chromium chromate species, which dehydrate completely at 513–610 K and decompose into chromate-covered α-Cr_2O_3 particles at 848–993 K.

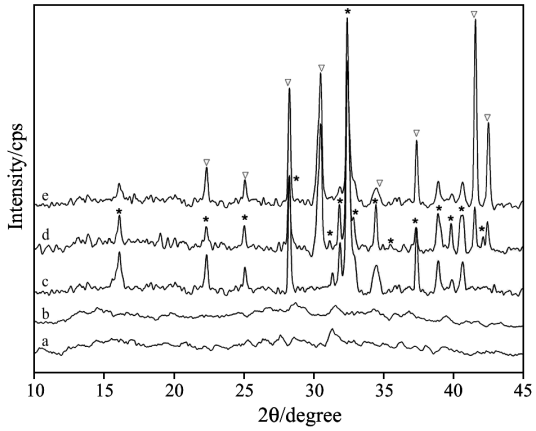

Fig. 4 X-ray diffraction pattern of sample with z=0.997 annealed at a – 573, b – 673, c – 823, d – 1003 and e – 1143 K; denotes the Bragg peaks: ∗ – $CrVO_4$–M, ▽ – $CrVO_4$–O

Chromium chromate species might be formed under chosen conditions of synthesis from partial oxidation of polynuclear complexes of Cr^{3+} ions in solution [36] or from oxidation of precipitated hydrous $Cr(OH)_3$ colloids under heat treatment in air. Crystallisation of Cr_2O_3 from amorphous chromium hydroxide in air with the involvement of higher oxidation states of chromium was reported by other authors as well [37–41]. Chromium chromate species may represent Cr^{3+}/Cr^{6+} mixed-valence structures based on octahedral $Cr^{3+}O_6$ and tetrahedral $Cr^{6+}O_4$ [42, 43]. This correlates with the results of our XPS measurements (not reported here), which confirm the presence of 34.51% of chromium in the Cr^{6+} oxidation state for preparation with z=3.049.

In accordance with the findings of Fouad *et al*. [44] and Rode *et al*. [42], the DTA-TG effects observed might encompass the release of oxygen and formation of bulk noncrystalline polychromate ($Cr_{1+x}O_{4+3x}^{2-}$) at ca. 848 K, which decomposes into nonstoichiometric γ-Cr_2O_{3+x} phase near 903 K. The noncrystalline γ-Cr_2O_{3+x} loses excess oxygen near 973 K giving rise to crystalline α-Cr_2O_3 and noncrystalline chromate species probably restricted to the surface of microcrystalline chromia particles. As it was shown [44–46], the dispersed chromates thus formed are thermally stable both in reducing and oxidising atmospheres up to 1273 K. Indeed, the crystalline α-Cr_2O_3 was not detected by our XRD measurements up to 1243 K indicating high thermal stability of the dominating intermediate chromate species, which do not assume a bulk crystalline structure [44].

With the further increase of chromium content ($z\geq3$) the described endothermic effects associated with the dissociative decomposition of intermediate

CrO_x phases shift to the lower temperatures (Fig. 1e) and crystalline Cr_2O_3 eventually forms at about 766 K. XRD results confirm that preparations with $z \geq 3$ heat treated at 865 K consist of mixture of Cr_2O_3 and $CrVO_4$–M phases. Exothermic peak at ca. 763 K corresponding to the crystallisation of $CrVO_4$–M is not resolved any more due to overlapping with the dominating endotherm corresponding to the transformation of noncrystalline γ-Cr_2O_{3+x} to crystalline α-Cr_2O_3, which takes place in the same temperature interval.

General considerations

Results of the thermoanalytical investigations as well as of X-ray diffraction analysis confirm that using the synthesis procedure applied [18], three hydrated phases were obtained: microcrystalline $V_{1-x}Cr_xO_y \cdot nH_2O$, where $x<0.063$ and $4.4<n<8$ ($z<0.067$) and amorphous $Cr_2V_4O_{13} \cdot 4H_2O$ ($z=0.5$) and $CrVO_4.H_2O$ ($z=1$). These hydrated oxides are the precursors of three crystalline anhydrous compounds: phase $V_{1-x}Cr_xO_y$, which is closely related to the orthorhombic V_2O_5, $Cr_2V_4O_{13}$ and monoclinic $CrVO_4$–M. It follows from the data obtained that $V_{1-x}Cr_xO_y$ and $Cr_2V_4O_{13}$ are in stable equilibrium up to 903 K and at $0.067< z \leq 0.5$, whereas $Cr_2V_4O_{13}$ and $CrVO_4$ coexist at $0.5 \leq z \leq 1$.

$Cr_2V_4O_{13}$ starts to decompose in the solid-state at 1033 K, while $V_{1-x}Cr_xO_y$ is stable up to 928 K. Walczak *et al*. [31] and Touboul *et al*. [12] reported the decomposition temperature of $Cr_2V_4O_{13}$ to be 913 and 903 K, respectively. Our XRD measurements, however, clearly showed the presence of $Cr_2V_4O_{13}$ phase for samples with Cr/V ratio in the range of $0.091 \leq z \leq 0.5$ heat treated up to 1033 K. Consistently, thermal effect at ca. 1033 K related to the incongruent melting of $Cr_2V_4O_{13}$ was recorded on the DTA curves for all samples in this range of composition. The presence of both endothermic effects at 918 and 1013 K on the DTA curves given by Walczak *et al*. for $Cr_2V_4O_{13}$ phase indicates that their preparation consisted of a mixture of phases and was not an individual compound $Cr_2V_4O_{13}$. On the other hand, exothermic peak at 903 K assigned by Touboul *et al*. [12] to the decomposition of $Cr_2V_4O_{13}$ phase might have some other origin (e.g. related to the melting of an eutectic mixture) as it was recorded for the preparation with a chemical composition of 33 mol% V_2O_5, which is markedly different from formula of $Cr_2V_4O_{13}$ phase (66 mol% V_2O_5).

The experimental results suggest that the large symmetrical and well-shaped endotherm at 903 K observed for samples with $0.067 \leq z < 0.5$ indicates formation of an eutectic mixture between $V_{1-x}Cr_xO_y$ and $Cr_2V_4O_{13}$ phases with $Cr_2V_4O_{13}$ content not exceeding 8 mol% of the compound. The exact composition of the eutectic mixture might be further verified by preparing and studying the thermal behaviour of the samples with Cr/V ratio in the range of $0.067<z<0.091$, where the abrupt shift of the large endotherm at 928 K ($z \leq 0.067$) to 903 K ($0.091 \leq z < 0.5$) was observed to occur.

Also it should be noted that application of soft chemistry methods often involves or/and results in formation of mixed valence polyoxovanadates [47–52]; the presence of V^{4+} species while applying peroxovanadate route has been reported and discussed in the literature [53–55]. Vanadium oxide bronzes, $M_xV_2O_5$ are known to contain vanadium in V^{4+} and V^{5+} formal oxidation states as well [56]. In the present study the presence of small amount of V^{4+} in the $V_{1-x}Cr_xO_y$ phase was evidenced from chemical redox titration. Therefore the $V_{1-x}Cr_xO_y$–$Cr_2V_4O_{13}$ system is likely to be considered as a binary intersection of the ternary system V_2O_5–V_2O_4–Cr_2O_3, phase diagram of which has not been unambiguously defined so far [57].

As far as V_2O_5–Cr_2O_3 system is concerned, discrepancies between the literature data have been found as regards the composition and melting point of the eutectic mixture formed in this system [17, 30–35]. The results of the present study imply that in V_2O_5–Cr_2O_3 system an eutectic exists rather between $Cr_2V_4O_{13}$ and V_2O_5 than between $CrVO_4$ (resulted from decomposition of $Cr_2V_4O_{13}$ phase) and V_2O_5, as was proposed earlier [31].

Conclusions

By using new aqueous method of synthesis, three hydrated phases were obtained: microcrystalline $V_{1-x}Cr_xO_y \cdot nH_2O$, were $x<0.063$ and $4.4<n<8$ and amorphous $Cr_2V_4O_{13} \cdot 4H_2O$ and $CrVO_4 \cdot H_2O$. Upon heating, these oxides have transformed to three anhydrous amorphous phases, which are precursors of three crystalline compounds: (*i*) phase $V_{1-x}Cr_xO_y$ ($z<0.067$), which is closely related to the orthorhombic V_2O_5, (*ii*) $Cr_2V_4O_{13}$ and (*iii*) monoclinic $CrVO_4$–M. Phase $V_{1-x}Cr_xO_y$ is likely to belong to the ternary system V_2O_5–V_2O_4–Cr_2O_3. $V_{1-x}Cr_xO_y$ and $Cr_2V_4O_{13}$ are in stable equilibrium up to 903 K and at $0.067<z \leq 0.5$, whereas $Cr_2V_4O_{13}$ and $CrVO_4$ coexist at $0.5 \leq z \leq 1$. Results obtained could contribute to the refinement of the phase diagrams for V_2O_5–Cr_2O_3 and V_2O_5–V_2O_4–Cr_2O_3 systems.

Acknowledgements

The support from the Hungarian Science Foundation (OTKA project no. M-027367) is greatly appreciated.

References

1 C. L. Thomas, Catalytic Processes and Proven Catalysts, Academic Press, New York 1970.
2 C. Pradier, F. Rodrigues, P. Marcus, M. Landau, M. Kaliya, A. Gutman and M. Herskowitz, Appl. Catal. B: Environmental, 27 (2000) 73.
3 H. Bosch and F. Janssen, Catal. Today, 2 (1988) 369.
4 R. Mariscal, M. Galan-Fereres, J. Anderson, L. Alemany, J. Palacios and J. Fierro, Environmental Catalysis; Eds SCI, Rome 1995, p. 223.
5 S. De Rossi, G. Ferraris, S. Fermiotti, A. Cimini and V. Indovina, J. Appl. Catal. A: General, 81 (1992) 113.
6 P. Wittgen, C. Groeneveld, P. Zwaans, H. Morgenstern, A. Van Heughten, C. Van Heumen and G. Schuit, J. Catal., 77 (1982) 360.
7 Y. Iwasawa and S. Ogasawa, Chem. Lett., 8 (1980) 127.
8 Y. Iwasawa, J. Mol. Catal., 17 (1982) 93.
9 S. De Rossi, G. Ferraris, S. Fremiotti, A. Cimino and V. Indovina, Appl. Catal., 81 (1992) 113.
10 P. Soudan, J. P. Pereira-Ramos, J. Farcy, G. Gregoire and N. Baffier, Solid State Ionics, 135 (2000) 291.
11 G. Gregoire, N. Baffier, A. Kahn-Harari and J. C. Badot, J. Mater. Chem., 8 (1998) 2103.
12 M. Touboul and K. Melghite, J. Mater. Chem., 5 (1995) 147.
13 S. Denis, E. Baudrin, M. Touboul and J. M. Tarascon, J. Electrochem. Soc., 144 (1997) 4099.
14 J. Amiel, D. Oliver and M. Dessolin, C. R. Hebd. Seances Acad. Sci., 264 (1967) 1045.
15 M. Kruchinina, A. Ivakin, L. Chaschina, O. Koryakova and V. Kozlov, Zh. Neorg. Khim., 38 (1993) 762.
16 D. Oliver and P. Rabette, C. R. Hebd. Seances Acad. Sci., 265 (1967) 1451.
17 D. Oliver and B. Combe, C. R. Acad. Sci., Paris, 267 (1968) 877.
18 O. Pozdnyakova, E. Kuzmann and L. Szirtes, Solid State Ionics, 161 (2003) 301.
19 Z. Klencsar, Personal communication.
20 J. Kristóf, J. Inczédy, J. Paulik and F. Paulik, J. Thermal Anal., 37 (1991) 111.
21 M. Hibino, M. Ugaji, A. Kisgimoto and T. Kudo, Solid State Ionics, 79 (1995) 239.
22 C. J. Fontenot, J. W. Wiench, G. L. Schrader and M. Pruski, J. Am. Chem. Soc., 124 (2002) 8435 and references therein.
23 L. Abello and C. Pomier, J. Chem. Phys. Phys.-Chem. Biol., 80 (1983) 373.
24 L. Abello, E. Husson, Y. Repelin and G. Lucazeau, J. Solid State Chem., 56 (1985) 379.
25 V. L. Volkov, G. S. Zakharova, V. G. Zubkov and A. A. Ivakin, Zh. Neorg. Khim., 31 (1986) 378.
26 V. L. Volkov, G. S. Zakharova and A. A. Ivakin, Zh. Neorg. Khim., 30 (1985) 1443.
27 L. Dupont, D. Larcher and M. Touboul, J. Solid State Chem., 143 (1999) 41.
28 L. Dupont and M. Sundberg, J. Solid State Chem., 136 (1998) 284.
29 O. Pozdnyakova, E. Kuzmann and L. Szirtes, unpublished data.
30 A. Burdese, Ann. Chem., 47 (1957) 97.
31 J.Walczak and E. Filipek, J. Thermal Anal., 35 (1989) 69.
32 J. Aminel, D. Colaitis and D. Oliver, C. R. Acad. Sci., Paris, 263 (1966) 224.
33 R. C. Kerby and J. R. Wilson, Can. J. Chem., 51 (1973) 1032.
34 S. M. Tsheshnickii, A. A. Fotiev and L. L. Surat, Zh. Neorg. Khim., 28 (1983) 2699.
35 E. C. Compleston, M. Y. Simons and B. Barham, J. Br. Ceram. Soc., 76 (1977) 68.
36 M. Pourbaix, Atlas of electrochemical equilibria in aqueous solutions, Pergamon Press, 1966.
37 J. D. Carruthers, K. S. W. Sing and J. Fenetry, Nature, London, 213 (1967) 66.
38 S. Music, M. Maljkovic, S. Popovic and R. Trojko, Croatica Chim. Acta, 72 (1999) 789.
39 S. L. M. Schroeder. G. D. Moggridge, T. Rayment and R. M. Lambert, J. Phys. IV France, 7 (1997) C2 923.
40 S. Labus, A. Małecki and R. Gajerski, J. Therm. Anal. Cal., 74 (2003) 13.
41 A. Małecki, B. Małecka, R. Gajerski and S. Labus, J. Therm. Anal. Cal., 74 (2003) 135.
42 T. V. Rode, Oxygen compounds of chromium catalysts, Izd. Akad. Nauk. SSSR, Moscow 1962.
43 B. L. Chamberland, Solid State Mater. Sci., 7 (1997) 1.
44 N. E. Fouad, S. A. Halawy, M. A. Mohamed and M. I. Zaki, Thermochim. Acta, 329 (1999) 23.
45 N. E. Fouad, H. Knozinger and M. I. Zaki, Z. Phys. Chem. Neue Folge, 171 (1991) 75.
46 M. I. Zaki, N. E. Fouad, G. C. Bond and S. F. Tahir, Thermochim. Acta, 285 (1996) 167.
47 N. Gharbi, C. Sanchez and J. Livage, Inorg. Chem., 21 (1982) 2758.
48 J. Livage, M. Henri and C. Sanchez, Inorg. Solid State Chem., 18 (1988) 259.
49 P. Barboux, D. Gourier and J. Livage, Colloids Surf., 11 (1984) 119.
50 J. Bullot, P. Cordier and O. Gallais, J. Non-Cryst. Solids, 68 (1984) 123.
51 G. A. Pozarnsky and A. V. McCormick, Chem. Mater., 6 (1994) 380.
52 D. K. Walanda, R. C. Burns, G. A. Lawrance and E. I. Nagy-Felsobuki, Inorg. Chim. Acta, 305 (2000) 11.
53 V. L. Volkov, G. S. Zakharova, A. P. Palkin and A. A. Ivakin, Neorg. Mater., 23 (1987) 992.
54 M. Bonchio, V. Conte, F. Difuria, G. Modena and S. Moro, Inorg. Chem., 33 (1994) 1631.
55 C. J. Fontenot, J. W. Wiench, M. Pruski and G. L. Schrader, J. Phys. Chem. B, 104 (2000) 11622.
56 V. L. Volkov, Intercalated compounds of vanadium oxides, Izd. Akad. Nauk. SSSR, Sverdlovsk 1987.
57 J. Galy, A. Casalot, J. Darriet and P. Hagenmuller, Bulletin de la Société Chim. De Fr., 1 (1967) 227 and references therein.

Received: March 30, 2005
In revised form: July 20, 2005

DOI: 10.1007/s10973-005-7025-9